







RESEARCH ARTICLE

10.1029/2021AV000431

Widespread Mismatch Between Phenology and Climate in Human-Dominated Landscapes

Yiluan Song¹ , Christopher J. Zajic¹, Taehee Hwang² , Christopher R. Hakkenberg³ , and Kai Zhu¹ 

¹Department of Environmental Studies, University of California, Santa Cruz, CA, USA, ²Department of Geography, Indiana University, Bloomington, IN, USA, ³School of Informatics, Computing & Cyber Systems, Northern Arizona University, Flagstaff, AZ, USA

Key Points:

- Rapidly shifting vegetation phenology has not kept pace with the recent climate change
- Climate-phenology mismatch is more pronounced in human-dominated landscapes with increasing human population density

Supporting Information:

Supporting Information may be found in the online version of this article.

Correspondence to:

Y. Song and K. Zhu,
ysong67@ucsc.edu;
kai.zhu@ucsc.edu

Citation:

Song, Y., Zajic, C. J., Hwang, T., Hakkenberg, C. R., & Zhu, K. (2021). Widespread mismatch between phenology and climate in human-dominated landscapes. *AGU Advances*, 2, e2021AV000431. <https://doi.org/10.1029/2021AV000431>

Received 8 MAR 2021

Accepted 16 SEP 2021

Peer Review The peer review history for this article is available as a PDF in the Supporting Information.

Author Contributions:

Conceptualization: Yiluan Song, Christopher J. Zajic, Taehee Hwang, Christopher R. Hakkenberg, Kai Zhu
Methodology: Yiluan Song, Christopher J. Zajic, Taehee Hwang, Christopher R. Hakkenberg, Kai Zhu
Supervision: Kai Zhu
Writing – original draft: Yiluan Song, Christopher J. Zajic, Taehee Hwang, Christopher R. Hakkenberg, Kai Zhu
Writing – review & editing: Yiluan Song, Christopher J. Zajic, Taehee Hwang, Christopher R. Hakkenberg, Kai Zhu

Abstract Plants track changing climate partly by shifting their phenology, the timing of recurring biological events. It is unknown whether these observed phenological shifts are sufficient to keep pace with rapid climate changes. Phenological mismatch, or the desynchronization between the timing of critical phenological events, has long been hypothesized but rarely quantified on a large scale. It is even less clear how human activities have contributed to this emergent phenological mismatch. In this study, we used remote sensing observations to systematically evaluate how plant phenological shifts have kept pace with warming trends at the continental scale. In particular, we developed a metric of spatial mismatch that connects empirical spatiotemporal data to ecological theory using the “velocity of change” approach. In northern mid-to-high-latitude regions (between 30–70°N) over the last three decades (1981–2014), we found evidence of a widespread mismatch between land surface phenology and climate where isolines of phenology lag behind or move in the opposite direction to the isolines of climate. These mismatches were more pronounced in human-dominated landscapes, suggesting a relationship between human activities and the desynchronization of phenology dynamics with climate variations. Results were corroborated with independent ground observations that indicate the mismatch of spring phenology increases with human population density for several plant species. This study reveals the possibility that not even some of the foremost responses in vegetation activity match the pace of recent warming. This systematic analysis of climate-phenology mismatch has important implications for the sustainable management of vegetation in human-dominated landscapes under climate change.

Plain Language Summary Plants are expected to track warming climate partly by shifting their phenology, the timing of recurring biological events. Despite numerous reports on phenological shifts driven by climate change, it is unknown whether these observed shifts are sufficient to keep pace with rapid warming trends at large spatial scales. It is even less clear how human activities contribute to the emergent climate-phenology mismatch. Using global remote sensing data, we employed a novel approach to systematically evaluate how plant phenological shifts have kept pace with warming trends at a continental scale. We found a net lag between phenological shift and climate change, which increases with population density, suggesting a relationship between human activities and the decoupling of phenology dynamics and climate variation. Results were corroborated with independent ground observations that show how the mismatch of spring phenology increases with human population density for several plant species. This systematic analysis of climate-phenology mismatch informs the sustainable management of vegetation in human-dominated landscapes under climate change.

1. Introduction

Phenology, the timing of recurring biological events, is nature's calendar, and changes in vegetation phenology are known to be among the most sensitive responses to ongoing climate change (Parmesan & Yohe, 2003). Evidence clearly shows warming-driven shifts in vegetation phenology at the global scale, such as earlier greenup and later senescence (Laskin et al., 2019; Menzel et al., 2020; W. Zhu et al., 2012). However, changes in phenology may fail to keep pace with warming trends (Duputié et al., 2015), possibly due to limited plasticity (B. A. Richardson et al., 2017), constraints due to photoperiod (Fu, Piao, et al., 2019; Fu, Zhang, et al., 2019), moisture (Peng et al., 2019; Wheeler et al., 2015), and unfulfillment of chilling requirements (Fu et al., 2015). Such climate-phenology seasonal mismatches can reduce individual fitness (A. D. Richardson et al., 2018), constrain

© 2021. The Authors.

This is an open access article under the terms of the [Creative Commons Attribution-NonCommercial License](https://creativecommons.org/licenses/by/4.0/), which permits use, distribution and reproduction in any medium, provided the original work is properly cited and is not used for commercial purposes.

species distributions (Morin et al., 2008), and drive biological invasions (Fridley, 2012). There is, however, little consensus on the existence and magnitude of climate-phenology mismatches.

Phenological mismatch, or the desynchronization in the timing of critical biotic and abiotic events, has long been discussed. The Cushing match-mismatch hypothesis (Cushing, 1969), for example, postulates that any change to the relative timing between consumers' activity and resource availability will lead to a "mismatch." Though this concept has mainly been applied to interacting species, we use it here in a broader sense to describe plant activity under favorable climatic conditions (Ovaskainen et al., 2013; Soolanayakanahally et al., 2013). Despite abundant evidence of shifting phenology and the sensitivity of phenology to climate change, the quantification of phenological mismatch remains challenging, partly due to the lack of a baseline from before the onset of anthropogenically driven climate change (Kharouba & Wolkovich, 2020). Such disconnects between ecological data and theory hinder our ability to understand the mechanisms and consequences of climate change at a large scale.

Human activities, particularly active management of croplands, pastures, and timberlands, have drastically changed land surface phenology. Possible pathways include modifying environmental conditions such as moisture and temperature (Kariyeva & van Leeuwen, 2012; Roetzer et al., 2000), changing vegetation cover and species composition (Buyantuyev & Wu, 2012), or altering natural disturbance regimes (Andela et al., 2017). However, it is unclear how these factors have been influencing emergent climate-phenology mismatches. On the one hand, in urban heat islands (Li et al., 2017) and adaptively managed agricultural systems (Bai et al., 2019), earlier greenup and subsequent longer growing seasons with time might promote synchrony between phenological shifts and warming. On the other hand, political or economic factors might lead to a decoupling between phenology and climate, such as the de-intensification of agricultural irrigation during wars (de Beurs & Henebry, 2008) and the change in crop types in response to policies and markets (Zhang et al., 2019). Despite the contributions of these local studies, we do not yet know how these results can be generalized to larger extents.

To systematically quantify long-term climate-phenology mismatch in both human-dominated (possessing human residence and intense land use) and natural landscapes at global scales, we first seek to establish a generalizable definition of the concept. We define phenological mismatch as the deviation between actual phenological response and expected phenological response based on historical phenology-environment relationships. This definition is deeply rooted in ecology. For example, Reed et al. (2013) defined the optimal egg-laying date of great tits to be 30 days before the date of peak food abundance. Their breeding phenology is expected to shift at the same pace as the timing of food abundance, but the actual breeding may be earlier or later, therefore potentially lowering the fitness of these birds. There can be multiple ways to quantify phenological response under this general definition. In this study, we develop a specific metric of spatial mismatch: the deviance between actual and expected movement in phenological isolines, where the expected movement corresponds to the movement of climatic isolines. The pace of geographic movement along the isoline over time (Loarie et al., 2009) is established as the velocity of change (Burrows et al., 2011) (Figure 1). Numerous studies have used this approach, to assess the pace of climate change (Burrows et al., 2011; Loarie et al., 2009), and to compare climate change with changes in species distribution (Burrows et al., 2011; Hamann et al., 2015; Lenoir et al., 2020) and productivity (Huang et al., 2017). This approach has also been used to compare changes in phenological and meteorological variables at an annual scale (O'Leary, 2020).

Our generalized definition and quantification method enable large-scale measurement of phenological mismatch using remote sensing data. Remote sensing data offers an excellent opportunity to examine the climate-phenology mismatch due to the extensive temporal and spatial coverage. We used a temporally and spatially contiguous remotely sensed land surface phenology (LSP) data set (VIPPHEN EVI2 Phenology data product v. 4.1) (Didan & Barreto, 2016) in this study. We first tested the hypothesis that shifts in vegetation phenology, characterized by remotely sensed LSP, have not been keeping pace with warming trends in mid-to high-latitudes in the Northern Hemisphere (between 30–70°N) over the past three decades (1981–2014). We further tested the hypothesis that climate-phenology mismatch is more pronounced in anthropogenically impacted regions than in natural landscapes. We acknowledge that remote sensing data are limited in their spatial resolution and the ability to reflect ground-observed phenological events. Therefore, in addition, we employed independent ground observations to analyze the possible anthropogenic influence on the mismatch of spring phenology in several plant species. We aim to provide insights on the effect of anthropogenic activity on climate-phenology mismatch at a global scale under ongoing unprecedented rates of climate and land use change. Resolving these questions hold the potential to inform future sustainable management of croplands, pastures, and timberlands.

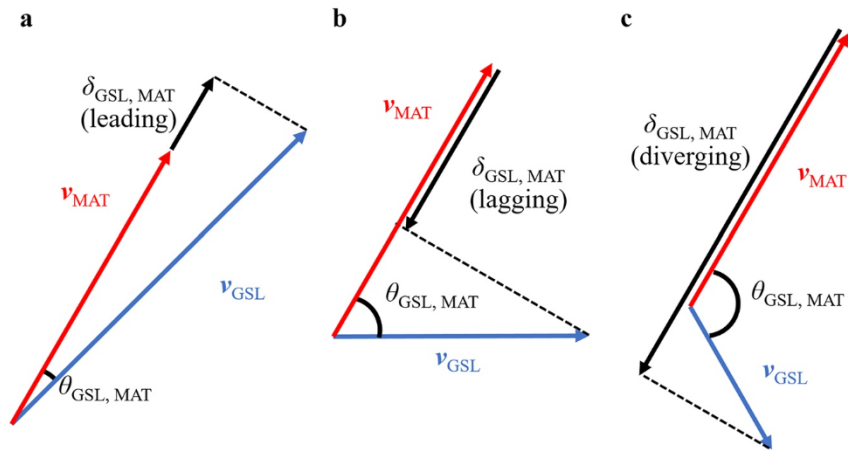


Figure 1. Schematic diagram showing three scenarios of climate tracking and the corresponding climate-phenology metrics. The velocity of mean annual temperature change, v_{MAT} (km yr^{-1}) and the velocity of growing season length change, v_{GSL} (km yr^{-1}) at a location were compared using the difference in two velocity directions, $\theta_{GSL, MAT}$ ($^{\circ}$) and the spatial mismatch, $\delta_{GSL, MAT}$ (km yr^{-1}). (a) A positive $\delta_{GSL, MAT}$ and a positive $\theta_{GSL, MAT}$ characterizes a leading mismatch; (b) A negative $\delta_{GSL, MAT}$ and a positive $\theta_{GSL, MAT}$ characterizes a lagging mismatch; (c) A negative $\delta_{GSL, MAT}$ and a negative $\theta_{GSL, MAT}$ characterizes a diverging mismatch.

2. Materials and Methods

2.1. Remote Sensing Analyses

2.1.1. Land Surface Phenology, Climate, Land Use, and Human Population Density Data

For latitudes between 30–70°N, we quantified the velocities of mean annual temperature (MAT) and growing season length (GSL), defined by the period between greenup and senescence, from 1981 to 2014. We chose to focus on the mid-to high-latitude Northern Hemisphere because of its high vegetation coverage and strong seasonality (X. Wang et al., 2019). In this area, GSL is highly correlated to MAT, suggesting a strong temperature control on phenology (Figure S1 in Supporting Information S1). We retrieved near-surface temperature data from 1981 to 2014 using the Climate Research Unit (CRU) time-series (TS) data set v. 4.03 (Harris et al., 2014). This data set reports monthly climatic variables from 1901 to 2018 at a 0.5-degree resolution, interpolated from meteorological station observations. We calculated the mean annual temperature (MAT) by taking the mean of near-surface temperatures of all months each year. We employed the VIPPHEN EVI2 Phenology data product v. 4.1 (Didan & Barreto, 2016) to obtain the satellite-observed LSP, represented by growing season length (GSL) in the present study. This data product provides reliable phenological metrics at a 0.05-degree resolution, derived from modified Enhanced Vegetation Index 2 (EVI2) using an adapted Half-Maximum Vegetation Index algorithm (White et al., 2009). EVI2 was calculated using surface reflectance data from the Advanced Very High Resolution Radiometer (AVHRR) (1981–1999) and Moderate Resolution Imaging Spectroradiometer (MODIS)/Terra MOD09 (2000–2014). Phenological data were subjected to two rounds of filtering in order to focus on areas with a single growing season and good data quality. Specifically, areas with multiple growing seasons (information provided in the phenology data product) were excluded as its phenology is often controlled by precipitation, rather than temperature, patterns (Ralhan et al., 1985). To eliminate the effects of data uncertainty, for each year only pixels with a single growing season and “excellent,” “good,” or “acceptable” data reliability were used, determined by the “number of seasons” and “data quality” fields in the data product. The raw LSP data were aggregated to a 0.5-degree resolution to match the spatial scale of the movement of temperature and phenology isolines over 34 years (Text S1 and Table S1 in Supporting Information S1).

To understand the relationship between anthropogenic factors and phenological responses, we used two datasets to qualitatively and quantitatively characterize anthropogenic land use. Qualitatively, the Anthromes v. 2 data set (Ellis et al., 2010) classifies land use for the year 2000. Quantitatively, we retrieved human population density for the year 2000 at a 0.5-degree resolution from the Gridded Population of the World data set v. 4 (Center For International Earth Science Information Network-CIESIN-Columbia University, 2018) as a proxy for anthropogenic

activities. Since we focus on the Northern Hemisphere, we cropped all global datasets to the latitudes between 30°N and 70°N.

2.1.2. Climate and Phenology Velocities

We quantified the velocity of MAT change, v_{MAT} ($\text{km}^\circ\text{yr}^{-1}$), and the velocity of GSL change, v_{GSL} (km yr^{-1}) by estimating the speed and direction of isoline movement, which implicitly makes use of a space-for-time substitution (Text S2, Figure S2, and Table S2 in Supporting Information S1). Based on these assumptions, we calculated instantaneous local velocities from the ratio of temporal ($^\circ\text{yr}^{-1}$ or $\text{day}^\circ\text{yr}^{-1}$) gradients in the 34 years, and spatial gradients ($^\circ\text{km}^{-1}$ or $\text{day}^\circ\text{km}^{-1}$) in grids of 0.5 for each variable (Burrows et al., 2011) using the *VoCC* package in R (Molinos et al., 2019):

$$v_{MAT} = \frac{dy}{dt} = \frac{\frac{dMAT}{dt}}{\frac{dMAT}{dy}}$$

$$v_{GSL} = \frac{dy}{dt} = \frac{\frac{dGSL}{dt}}{\frac{dGSL}{dy}}, \quad (1)$$

where t is time and y is space (distance with direction). The temporal gradient ($dMAT/dt$ or $dGSL/dt$) is the slope coefficient in the linear regression of the variable of interest with time. Pixels with fewer than 10 out of the 34 years of valid observations in either the MAT or GSL products were removed from analyses. The spatial gradient ($dMAT/dy$ or $dGSL/dy$) is the vector sum of the N–S and E–W gradients in a 3×3 pixel neighborhood, pointing in the direction of the decreasing variable of interest. When the temporal gradient is positive, the direction of the velocity (θ_{GSL} or θ_{MAT}) is in the same direction as that of the spatial gradient. When the temporal gradient is negative, the direction of velocity is the opposite of that of the spatial gradient. As velocity metrics are sensitive to spatial gradients, we acknowledge that high spatial heterogeneity in phenology may lead to slightly under-estimated v_{GSL} values, especially in human-dominated landscapes (Text S3, Figures S3 and S4 in Supporting Information S1).

To quantify how well the velocity of phenology change keeps pace with the velocity of temperature change, we took the directions of both vectors into account (Ordonez et al., 2016) and calculated two scalar metrics: the directional difference and relative pacing from two vector measures, v_{GSL} and v_{MAT} (Figure 1). First, we calculated the absolute difference in the directions of velocities, $\theta_{GSL,MAT}$, using

$$\theta_{GSL,MAT} = \min\left\{|\theta_{GSL} - \theta_{MAT}|, 360 - |\theta_{GSL} - \theta_{MAT}|\right\}, \quad (2)$$

where θ_{GSL} and θ_{MAT} are the directions of v_{MAT} and v_{GSL} , respectively, measured in degrees starting from the north. $\theta_{GSL,MAT}$ ranged from 0° to 180°, with smaller $\theta_{GSL,MAT}$ implying that GSL and MAT isolines move in more closely aligned directions. This metric describes how GSL and MAT are coupled in space, such that a $\theta_{GSL,MAT}$ smaller than 90° represents a positive alignment and a $\theta_{GSL,MAT}$ larger than 90° represents a negative alignment.

Second, we evaluated the pacing of phenology relative to climate, $\delta_{GSL,MAT}$ by projecting v_{GSL} onto v_{MAT} and subtracting by v_{MAT} (Figure 1), using

$$\delta_{GSL,MAT} = |v_{GSL}| \times \cos\theta_{GSL,MAT} - |v_{MAT}| \quad (3)$$

In addition to GSL, we also quantified the velocity of phenology change using the start of season (SOS) and end of season (EOS). Instead of MAT, we compared these velocities to the velocities of change in mean spring temperature (MST) (March to May) and mean fall temperature (MFT) (September to November), respectively.

2.1.3. Effects of Anthropogenic Land Use

We assessed the effects of anthropogenic activities on climate-phenology mismatch using two approaches. First, we compared four climate-phenology metrics (v_{MAT} , v_{GSL} , $\theta_{GSL,MAT}$ and $\delta_{GSL,MAT}$) between different land-use types based on the Anthromes data set (Ellis et al., 2010). The data set broadly classifies our study area into

“dense settlements,” “villages,” “croplands,” “rangelands,” “semi-natural,” and “wildlands,” with the first five types modified by anthropogenic activities to different extents. The “villages” and “dense settlements” categories were then consolidated into a larger land-use type that we call “settlements” and subsequently removed from the analysis (only 5% of all pixels analyzed) as these patches are usually on a smaller scale than the spatial resolution of this analysis (0.5 degree). We ranked the other four land-use types according to the median value of the climate-phenology metrics in each area. We compared the climate-phenology metrics in areas with anthropogenic land use to those in “wildlands” using one-way ANOVA with post-hoc Tukey HSD tests.

Second, we modeled how four climate-phenology metrics are correlated to both population density and latitude, in order to detect the underlying anthropogenic gradient in these metrics, while controlling for the latitudinal gradient. We log-transformed the velocities of change and logit-transformed the difference in directions, as an angle, to better account for their distributions and meet the normality assumption of linear regression:

$$\begin{aligned}
 v'_{\text{MAT}} &= \log(v_{\text{MAT}}) \\
 v'_{\text{GSL}} &= \log(v_{\text{GSL}}) \\
 \theta'_{\text{GSL,MAT}} &= \log\left(\frac{\theta_{\text{GSL,MAT}}}{180 - \theta_{\text{GSL,MAT}}}\right) \quad (4)
 \end{aligned}$$

All datasets were upscaled to a 5-degree resolution by taking the median value of all pixels, in order to reduce noise at the finer scale and focus on large-scale patterns in the regression analyses. The upscaled raster was then reprojected to an azimuthal equidistant projection centering at the north pole, so that the Euclidean distances between pixels could be calculated more accurately.

We adopted a Bayesian approach because of its flexibility in incorporating information on spatial structures empirically determined from the data to infer the effects of population density and latitude. Latitude (related to photoperiod) is a potential confounding factor as it may be correlated to the rate of warming, rate of phenological shift, and population density. Although phenological shift is strongly dependent on topography (Cornelius et al., 2013; Delpierre et al., 2009; Elmore et al., 2012; Hwang et al., 2011, 2014; A. D. Richardson et al., 2006; Vitasse et al., 2011), we do not include topographical variables like elevation as predictors, as they are implicitly accounted for in temperature (Figure S5 in Supporting Information S1). The elevational shift in phenological variables is expected to track that of temperature variables, as is predicted by Hopkin's law (Hopkins, 1918). Therefore elevational shifts are reflected in our calculation of horizontal velocities of change, such as environmental lapse rates. We fitted Bayesian spatial linear regression models with exponential spatial correlation using the *spBayes* package in *R* (Finley et al., 2013) (see Text S4, Tables S3 and S4, Figures S6 and S7 in Supporting Information S1 for comparison with nonspatial models):

$$y(s) = \beta_0 + \beta_1 X_1(s) + \beta_2 X_2(s) + w(s) + \varepsilon$$

$$w(s) \sim N(0, K) \quad K_{ij} = \sigma^2 \exp(-\varphi \|s_i + s_j\|)$$

$$\varepsilon \sim N(0, \tau^2)$$

$$\begin{pmatrix} \beta_0 \\ \beta_1 \\ \beta_2 \end{pmatrix} \sim \text{MVN} \left[\begin{pmatrix} 0 \\ 0 \\ 0 \end{pmatrix}, \begin{pmatrix} 100 & 0 & 0 \\ 0 & 100 & 0 \\ 0 & 0 & 100 \end{pmatrix} \right]$$

$$\sigma^2 \sim \text{IG}(2, 2)$$

$$\varphi \sim \text{U} \left(-\frac{\log(0.05)}{100d}, -\frac{\log(0.05)}{0.01d} \right)$$

$$\tau^2 \sim \text{IG}(2, 0.1), \quad (5)$$

where the response variable y is ν'_{MAT} , ν'_{GSL} , $\theta'_{\text{GSL,MAT}}$, or $\delta_{\text{GSL,MAT}}$, the covariates X_1 and X_2 are human population density (on a logarithmic scale) and latitude, β_0 , β_1 , and β_2 are the coefficients for intercepts and covariates, s is the location of observation, and ε is the random error. The spatial random effect, \mathbf{w} , is determined by the spatial variance parameter σ^2 , the residual error variance τ^2 , the spatial decay parameter φ , and the Euclidean distance between locations i and j . We empirically determined the general form of the spatial correlation structure from the semivariograms of the residuals of the corresponding nonspatial linear regression models. We empirically estimated d , the effective range of spatial dependence, d (i.e., the distance at which the correlation drops to 0.05) is $-\log(0.05)/d$ (Finley et al., 2015), by fitting an exponential function to the semivariograms and calculating the range (i.e., the distance at which semivariogram meets asymptote). We calculated the interval of φ that corresponds to a wide interval of possible d , $(0.01 d, 100d)$. For all models, we used common choices of diffuse multivariate normal (MVN) priors on β , diffuse inverse gamma (IG) priors on τ^2 and σ^2 , and diffuse uniform (U) priors on φ (Finley et al., 2013).

We ran the Markov chain Monte Carlo (MCMC) sampler for 10,000 samples (Finley et al., 2013), discarding the first 5,000 samples as burn-in. We verified convergence and stability of estimates by visual inspection of the MCMC chains, their autocorrelation and partial autocorrelation functions, and summarized the medians and 95% credible intervals (CI) of β . For the three models with transformed response variables, the ν'_{MAT} , ν'_{GSL} , or $\theta'_{\text{GSL,MAT}}/180 - \theta_{\text{GSL,MAT}}$ change by β_1 percent for every percent increase in population density. We back-transformed and then interpreted the coefficients. All calculations and statistical analyses were conducted in *R* (v. 3.6.0, R Core Team., 2019).

2.2. Ground Observation Analyses

2.2.1. Ground-Observed Phenology Data

In addition to the remote sensing analyses, we used the USA National Phenology Network (USA-NPN) database (Elmendorf et al., 2016) to inform the climate-phenology mismatch on the ground level. In particular, we retrieved the site-specific onset of leaf-out activities, described as “breaking leaf buds,” “breaking needle buds,” “budburst,” “emergence above ground,” “emerging leaves,” “emerging needles,” “first leaf,” or “initial growth,” in the database. We also retrieved the growing degree days, maximum spring temperature, and minimum spring temperature associated with these phenometrics from the USA-NPN database. To control the data quality and to limit the scope of our analysis, we focused on the “calibration” species labeled in the database, which are monitored to provide patterns of plant phenophase responses across the US. We also filtered for species with more than 100 records.

2.2.2. Calculating Mismatch and Inferring Anthropogenic Effect

Due to the limited spatiotemporal coverage of ground observations, we were unable to calculate their velocity of change in phenology, and therefore the spatial climate-phenology mismatch. As an alternative, we fitted a climate-phenology model for each species, with the leaf-out day of year as the response, and three temperature variables (growing degree days, maximum spring temperature, and minimum spring temperature) as predictors. The absolute model predictive errors were taken as a measure of climate-phenology mismatch. This alternative method is conceptually consistent with our general definition of climate-phenology mismatch (the deviation between actual and expected phenological response) and hence consistent with the previous velocity method for the remote sensing analyses. Here, the assumption is that with close climate-phenology coupling, there should be a stable functional relationship between climate and phenology, and deviations from this relationship are signs of decoupling. Due to the limited sample size, we adopted a linear model structure and recognized the nonlinear relationships as a potential future research direction.

We strived to make the ground-based and remote sensing analyses as comparable as possible. For the ground observations, we tested the relationship between the prediction error (climate-phenology mismatch) and human population density (on a logarithmic scale) for each species. Latitude was included as a predictor to account for its potential confounding effect. Both designs are similar to Equation 5 in the remote sensing analyses. All calculations and statistical analyses were conducted in *R* (v. 3.6.0, R Core Team., 2019).

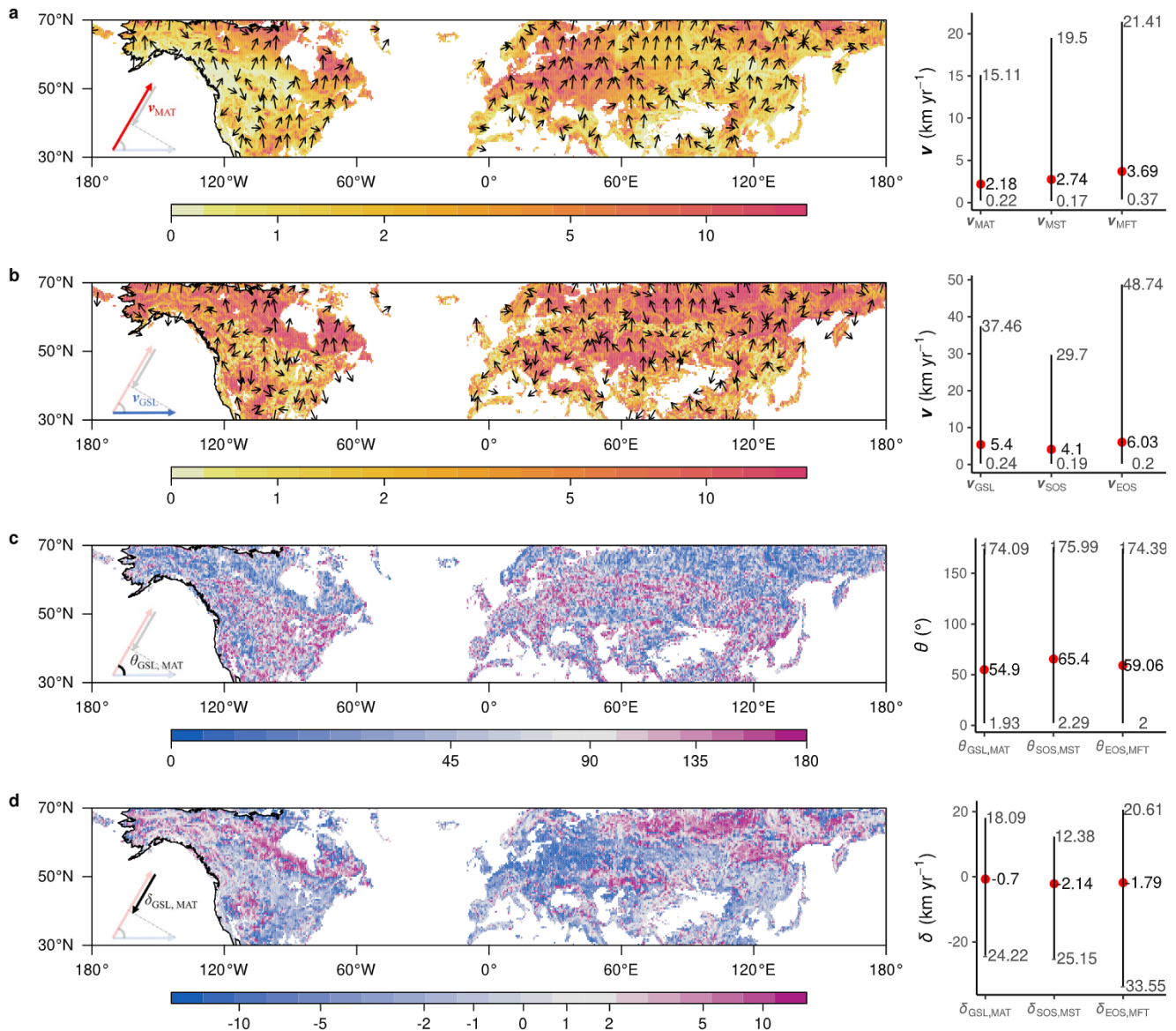


Figure 2. Spatial patterns of four climate-phenology metrics. (a) Velocity of mean annual temperature change, v_{MAT} (km yr⁻¹). (b) Velocity of growing season length change, v_{GSL} (km yr⁻¹). (c) Difference in direction, $\theta_{GSL,MAT}$ (°). (d) Pace of phenology change relative to climate, $\delta_{GSL,MAT}$ (km yr⁻¹). Color bars show the magnitude of each metric, with cutpoints chosen to divide the data into quantiles. For (a) and (b), the cutpoints were chosen based on pooled v_{MAT} and v_{GSL} , so that they are directly comparable. Arrows show the direction of the velocities of change in selected pixels. Inset figures depict how metrics were calculated (see more details in Figure 1). Panels on the right show the median and 95% intervals of climate-phenology metrics calculated using growing season length (GSL), start of season (SOS), end of season (EOS) as proxies for phenology, and using mean annual temperature (MAT), mean spring temperature (MST) and using mean fall temperature (MFT) as proxies for climate, respectively.

3. Results

3.1. Mismatches Between Velocities of Climate and Phenology

The isolines of climate and phenology show rapid movement in the study region (Figures 2a, 2b, and S8 in Supporting Information S1), with a median velocity of mean annual temperature change (v_{MAT}) of 2.2 km yr⁻¹ (95% CI: 0.2, 15.1 km yr⁻¹). There is considerable spatial heterogeneity in v_{MAT} , with higher v_{MAT} in high-latitude North America and Siberia and low v_{MAT} in western N. America and E. Asia. The direction of v_{MAT} is northward in the majority (78.3%) of the area, especially at high latitudes. The median velocity of growing season length change (v_{GSL}) is 5.4 km yr⁻¹ (95% CI: 0.2, 37.5 km yr⁻¹), which is more than twice that of v_{MAT} . Similar to the

spatial pattern observed for v_{MAT} , v_{GSL} is higher in high-latitude N. America and Siberia, but lower in eastern N. America and E. Asia. The directions of v_{GSL} are less consistent than those of v_{MAT} , with 61.4% of pixels indicating a northward direction, mainly at high latitudes.

There are wide discrepancies between the directions of v_{MAT} and v_{GSL} , as measured by $\theta_{GSL,MAT}$ (Figures 2c and S8 in Supporting Information S1), with 34.1% of pixels having a $\theta_{GSL,MAT}$ greater than 90° and a median $\theta_{GSL,MAT}$ of 54.9° (95% CI: 1.9, 174.1°). We find smaller $\theta_{GSL,MAT}$ values at high-latitudes (50° – 70° N) than those of mid-latitudes (30° – 50° N), with the largest $\theta_{GSL,MAT}$ values in eastern N. America, Europe, central Asia, and E. Asia. To quantify how well v_{GSL} kept pace with v_{MAT} , we calculated their spatial mismatch, $\delta_{GSL,MAT}$ (Figures 2d and Figure S8 in Supporting Information S1). A positive $\delta_{GSL,MAT}$ corresponds to v_{GSL} leading ahead of v_{MAT} (a leading mismatch), while a negative value corresponds to v_{GSL} lagging behind (a lagging mismatch) or being in the opposite direction (a diverging mismatch) (Figure 1). Overall, the combination of high v_{MAT} , low v_{GSL} , and large $\theta_{GSL,MAT}$ leads to a $\delta_{GSL,MAT}$ of -0.7 km yr^{-1} (95% CI: $-24.2, 18.1 \text{ km yr}^{-1}$), with negative $\delta_{GSL,MAT}$ values in 55.4% of the study area. The two velocities are similar between 50° – 70° N, but $\delta_{GSL,MAT}$ is highly negative between 30° – 50° N. Highly negative $\delta_{GSL,MAT}$ is observed in Europe and part of N. America, but $\delta_{GSL,MAT}$ is near-zero in E. Asia. Finally, some areas of Siberia and high-latitude N. America possess a positive $\delta_{GSL,MAT}$. The velocities of change and spatial mismatches calculated with remotely sensed phenology data are comparable to those calculated with field data in the order of magnitude.

Analyses of the climate tracking of spring and fall phenology offer similar, yet more nuanced understandings of climate-phenology coupling (Figure 2). The velocity of start of season (SOS), v_{SOS} (median 4.1 km yr^{-1} , 95% CI: 0.2, 29.7 km yr^{-1}) greatly exceeded the velocity of MST, v_{MST} (median 2.7 km yr^{-1} , 95% CI: 0.2, 19.5 km yr^{-1}), but there were large $\theta_{SOS,MST}$ (median 65.4° , 95% CI: $2.3^\circ, 176.0^\circ$) and $\delta_{SOS,MST}$ (median -2.1 km yr^{-1} , 95% CI: $-25.1, 12.4 \text{ km yr}^{-1}$). Similarly, the velocity of end of season (EOS), v_{EOS} (median 6.0 km yr^{-1} , 95% CI: 0.2, 48.7 km yr^{-1}) greatly exceeded the velocity of mean fall temperature (MFT), v_{MFT} (median 3.6 km yr^{-1} , 95% CI: 0.4, 21.4 km yr^{-1}), but there were large $\theta_{EOS,MFT}$ (median 59.1° , 95% CI: $2.0^\circ, 174.4^\circ$) and $\delta_{EOS,MFT}$ (median -1.8 km yr^{-1} , 95% CI: $-33.6, 20.6 \text{ km yr}^{-1}$). The climate-phenology metrics and their spatial patterns (Figures S9 and S10 in Supporting Information S1) are similar to those calculated using GSL and MAT. Nevertheless, we did notice that the spatial mismatch found with the growing season length (-0.7 km yr^{-1}) is generally weaker than those found in the spring (-2.1 km yr^{-1}) and in the fall (-1.8 km yr^{-1}), suggesting a stronger coupling between temperature and spring phenology.

3.2. Climate-Phenology Mismatches in Anthropogenic Landscapes

To examine possible anthropogenic influences on the climate-phenology mismatch, we compared four climate-phenology metrics (v_{MAT} , v_{GSL} , $\theta_{GSL,MAT}$, $\delta_{GSL,MAT}$) based on the five land-use types from the global anthropogenic biomes Anthromes 2 data (Ellis et al., 2010) (Figure 3). Croplands had the highest v_{MAT} , followed by wildlands, semi-natural, and rangelands. Croplands had the lowest v_{GSL} , greatest $\theta_{GSL,MAT}$, and lowest $\delta_{GSL,MAT}$. Semi-natural and rangelands were similar in these three metrics, while wildlands had the highest v_{GSL} , smallest $\theta_{GSL,MAT}$, and highest $\delta_{GSL,MAT}$. Notably, v_{GSL} outpaced v_{MAT} only in wildlands (positive $\delta_{GSL,MAT}$), but it lagged behind or moved in opposite directions in all anthropogenic land uses (negative $\delta_{GSL,MAT}$). Kolmogorov-Smirnov tests showed that statistical distributions of the four climate-phenology metrics in all anthropogenic land-use types were significantly different from those in the wildlands ($p < 0.001$). Nevertheless, the comparison across land use types might be confounded by the correlation between land use and latitude, which is addressed by a subsequent model to account for both.

We tested for a natural-anthropogenic gradient underlying climate-phenology mismatches by modeling the relationship between the four climate-phenology metrics and human population density (Center For International Earth Science Information Network-CIESIN-Columbia University, 2018) (Figure 4). One might argue that these relationships could be confounded by latitude, as population density, agricultural intensity, and agricultural practices might covary with the climate-phenology metrics along the latitudinal gradient. We used a Bayesian spatial model to explicitly account for a latitudinal trend and possible spatial autocorrelation in the response variables (Text S4 in Supporting Information S1). After accounting for these factors, we found that population density is significantly correlated with v_{GSL} and $\delta_{GSL,MAT}$ (Table S5 in Supporting Information S1). A 1% increase in human population density corresponds to a 0.15% reduction in v_{GSL} and a 0.69 km yr^{-1} increase in the lagging or

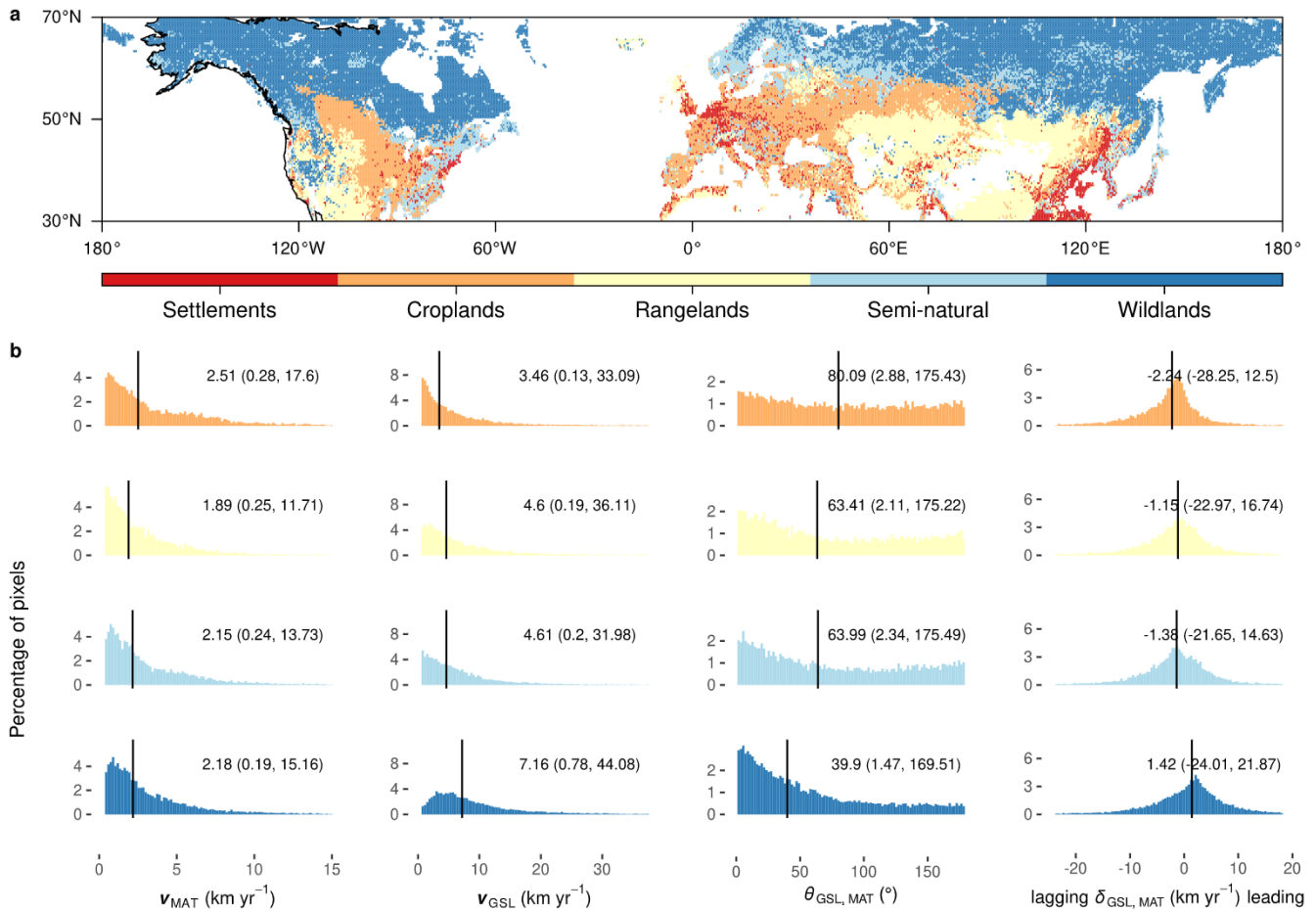


Figure 3. Climate-phenology metrics by land-use types. (a) Map of land-use types in 2000, based on the Anthromes 2 data (Ellis et al., 2010). Land uses were classified into five different types: settlements, croplands, rangelands, semi-natural, and wildlands. Settlements were excluded from the following comparisons as their small spatial scales might lead to inaccurate calculation of climate-phenology metrics. (b) Distributions of the velocity of mean annual temperature change, v_{MAT} (km yr⁻¹), the velocity of growing season length change, v_{GSL} (km yr⁻¹), the difference in direction, $\theta_{GSL, MAT}$ (°), and the pacing of phenology relative to climate, $\delta_{GSL, MAT}$ (km yr⁻¹) in five land-use types. Histograms are ranked based on the medians of the distributions in the land-use type (vertical lines). For v_{MAT} , v_{GSL} , and $\delta_{GSL, MAT}$, only values between 2.5% and 97.5% quantiles are presented in the histograms.

diverging mismatch between v_{GSL} and v_{MAT} . Despite the possible latitude-population correlation, latitude was not a significant predictor of $\delta_{GSL, MAT}$, highlighting the role of anthropogenic influence.

3.3. Ground-Observed Climate-Phenology Mismatches Along Population Gradients

In order to understand the natural-human gradient at finer spatial scales, we analyzed the ground-observed leaf-out dates of seven selected plant species. The median absolute predictive error, representing climate-phenology mismatch on the ground level, was 6.4 days (95% interval: 0.3–26.7 day). We again tested for the relationship between the absolute predictive error and the log-transformed human population density (Center For International Earth Science Information Network-CIESIN-Columbia University, 2018) (Figure 5). We found that human population density (on a logarithmic scale) was positively associated with the absolute predictive error in six out of seven species (coefficient 0.005–0.76) and negatively associated in only red maple (coefficient -0.02). The relationship was significant ($p < 0.05$) for common lilacs, which has the largest sample size. Overall, a 1% increase in human population density corresponds to a 0.28 day increase in the absolute predictive error ($p < 0.05$).

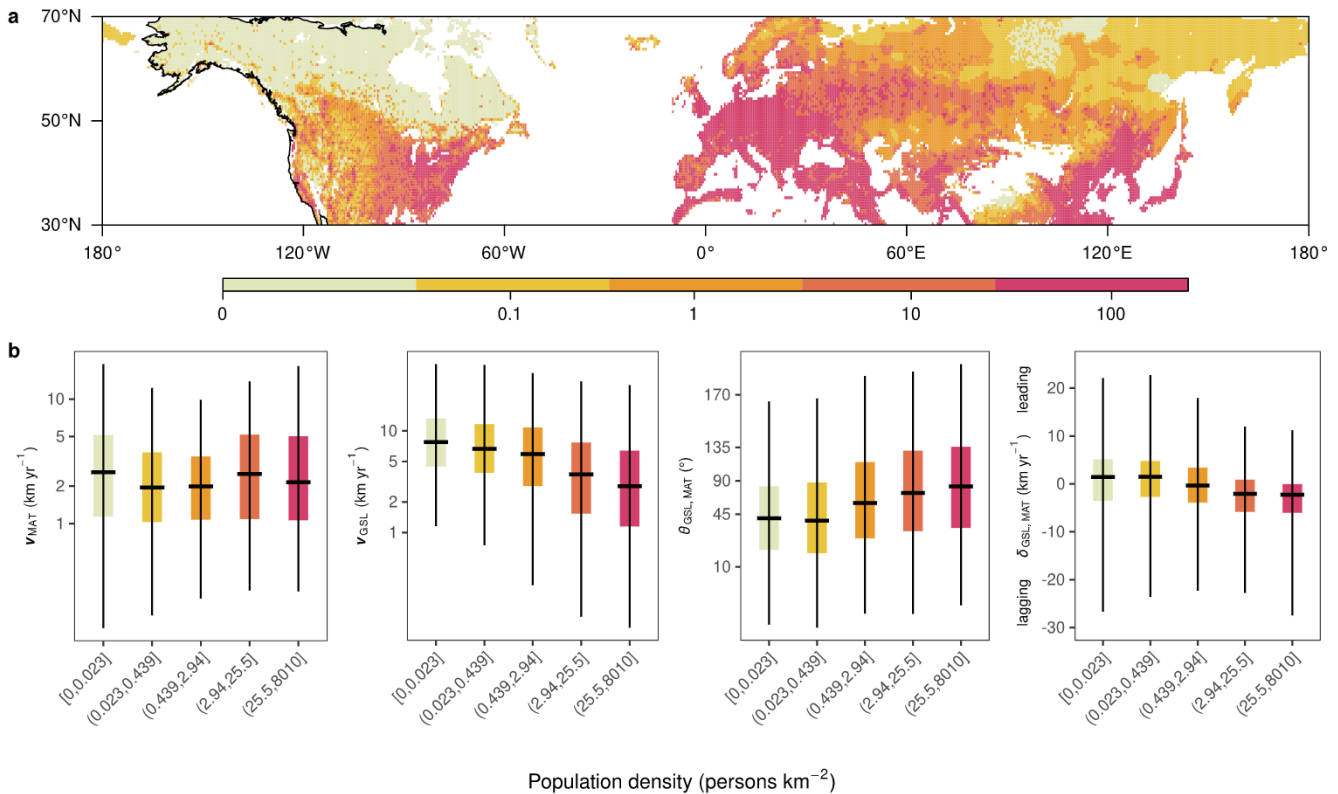


Figure 4. Relationship between population density and climate-phenology metrics. (a) Map of population density (persons km⁻²) in the study area in 2000 (Center For International Earth Science Information Network-CIESIN-Columbia University, 2018). Color shows the population density, with cutpoints chosen to divide the data into quantiles. (b) Velocity of mean annual temperature change, v_{MAT} (km yr⁻¹), velocity of growing season length change, v_{GSL} (km yr⁻¹), the difference in direction, $\theta_{GSL,MAT}$ (°), and the pacing of phenology relative to climate, $\delta_{GSL,MAT}$ (km yr⁻¹) in five quantiles of population density. The lower end of the whiskers, lower boundary of the boxes, middle of the boxes, higher boundary of the boxes, and the higher end of the whiskers are 0.025, 0.25, 0.5, 0.75, and 0.975 quantiles of the distributions, respectively. For visualization, the y-axis scales have been log-transformed for v_{MAT} and v_{GSL} , and logit-transformed for $\theta_{GSL,MAT}$.

4. Discussion

From our global analyses of remote sensing and ground-based data, we found that plant phenology does not perfectly track climate change, and that the mismatch is greater in human-dominated landscapes. Previous studies have found that the rapid advancement of spring phenology outpaces the shift in the seasonal timing of spring temperatures (Ovaskainen et al., 2013). Those results are partly supported by our finding of a leading mismatch between phenological shifts and temperature changes in natural landscapes (Figure 3). However, across the entire study area, there is an overall lagging or diverging spatial mismatch in mixed natural and anthropogenic landscapes. Several possible mechanisms explain why the movement of phenology isolines lags behind or is oriented in the opposite direction compared with those of temperature isolines, including insufficient phenotypic plasticity (Duputié et al., 2015), photoperiod limitations (Bauerle et al., 2012; Fu, Piao, et al., 2019; Fu, Zhang, et al., 2019; Körner & Basler, 2010; Zohner et al., 2016), and the interaction between warming and chilling requirements (Fu et al., 2015). These lags might also be explained by phenological response to factors other than temperature, such as drought stress (Peng et al., 2019) and CO₂ concentration (S. Wang et al., 2019). In the remote sensing analysis, the landscape-level lag may be additionally attributed to insufficient species compositional change (Helman, 2018). A possible explanation for the decoupling of phenology and climate is the decreasing sensitivity of vegetation phenology to temperature (Fu et al., 2015), but this mechanism is open to discussion because of known issues in the calculation of temperature sensitivity (Keenan et al., 2020). Plant functional types can be another factor that explains the outpacing phenology patterns in wildlands, especially in high-latitude regions dominated by shrublands, evergreen needleleaf forests, and grasslands (Text S5, Figure S11 in Supporting Information S1).

Phenology responds to multiple climatic factors in complex ways. We used MAT as a proxy for climate in this study and focused on temperate areas with distinct seasonality, where temperature is the main driver of phenology

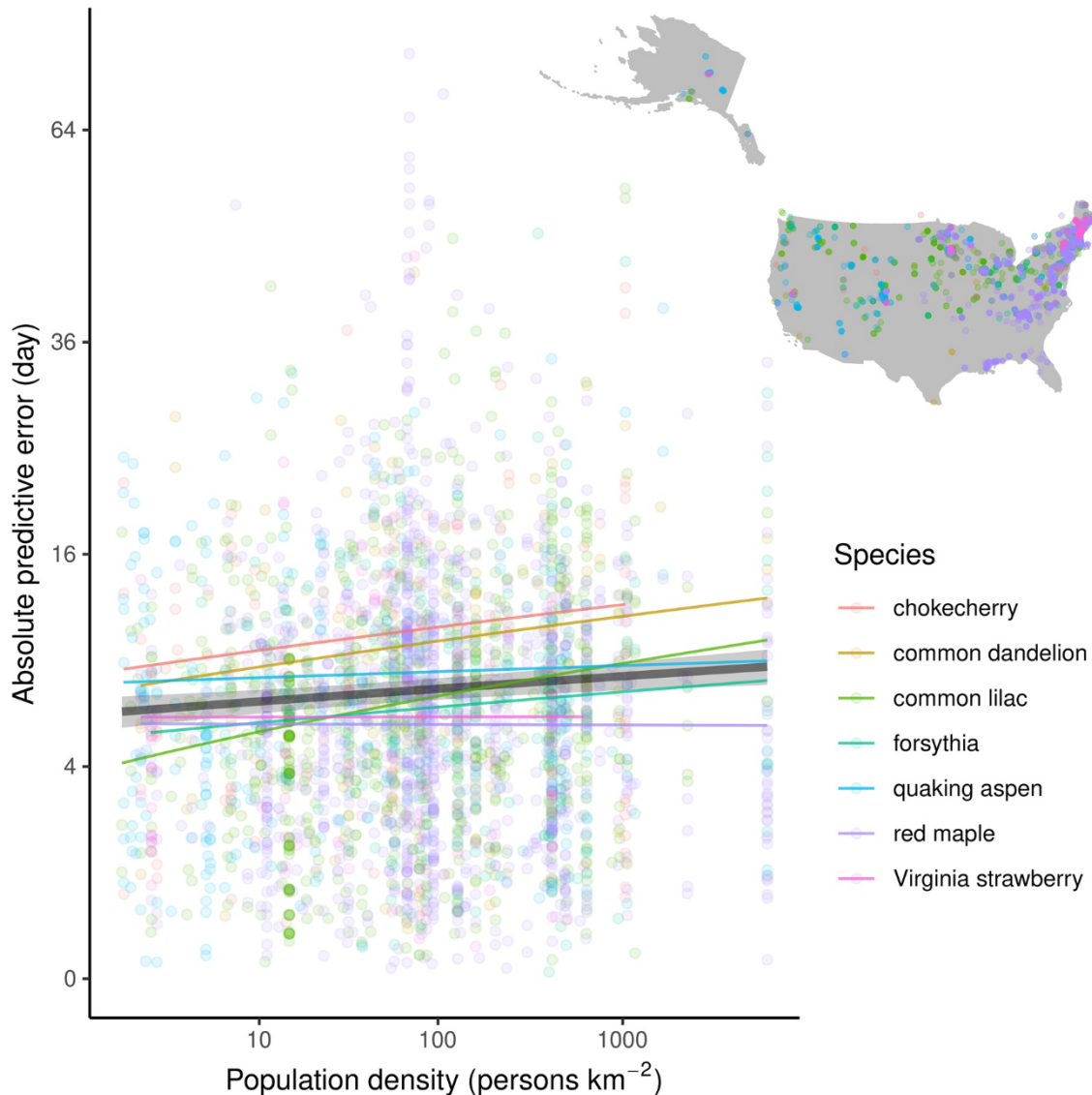


Figure 5. Anthropogenic influence on the ground-level climate-phenology mismatch calculated from the leaf-out dates of seven selected plant species in the USA-NPN database. Scatterplot shows the relationships between log-transformed human population density and absolute predictive error (day) between observed and model-predicted leaf-out dates. Black line and gray ribbon show the overall linear trend and 95% interval, respectively. Colored lines show the species-specific linear trends. Inset map shows the locations of observational sites with phenometrics on the leaf-out dates of the studied species.

(see a supplementary analysis using mean annual precipitation, Text S6 and Figure S12 in Supporting Information S1). However, we acknowledge that there are many ecosystems where phenology is driven by precipitation instead of temperature, particularly in grasslands (Miao et al., 2017). For example, warming-induced drought stress could delay greenup onset and advance senescence in temperate grasslands (Tao et al., 2008), whereas an increase in preseason precipitation often causes the opposite (Ren et al., 2018). Note that climate-phenology tracking is stronger in spring compared to the fall ($\delta_{\text{SOS,MST}}$ are generally closer to 0 compared to $\delta_{\text{EOS,MFT}}$ in Figure 2d), which can be interpreted as higher sensitivity of senescence to water stress or photoperiod than greenup. We therefore suggest future studies use multivariate vectors when calculating the velocity of change in climate and high-dimensional nonlinear models when calculating model predictive errors.

Our findings on phenological shifts can be situated in a broader context of ecological responses to climate change, including phenological, distributional, and physiological responses (Hällfors et al., 2021). Apart from plant phenology, recent studies on plant migration and productivity have also shown lags in biotic responses to climate change. For example, the velocity of climate change has been suggested to exceed optimistic estimates for plant

migration rates ($\sim 1 \text{ km yr}^{-1}$) in 28.8% of the globe (Loarie et al., 2009). This estimation was confirmed by a systematic analysis of forest inventory data, which revealed that the minimal northward expansion of tree ranges in the eastern US has failed to keep pace with climate change (K. Zhu et al., 2012). An analysis of changes in plant productivity suggests that the velocity of productivity change lags behind that of temperature change in 80% of the northern high latitudes (Huang et al., 2017). Altogether, these studies corroborate results from this analysis to reveal the possibility that not even some of the most rapid responses in vegetation activity match the pace of recent climate change.

Our study suggests that anthropogenic effects are closely associated with the desynchronization of land surface phenology and temperature. Despite intensive land management, croplands had one of the highest climate-phenology mismatches among all land uses, with strong warming trends often accompanied by shortened growing seasons (Figures 2b and 3b). The accuracy of remote sensing in detecting the phenology of crops has been validated with ground observations, such as the crop progress stages reported by the U.S. Department of Agriculture (USDA) National Agricultural Statistics Service (NASS) (Duncan et al., 2015; Gao et al., 2017; Peng et al., 2019; Sakamoto et al., 2005). Crop phenologies have complex responses to climate change. On the one hand, the established climate-phenology coupling may be disrupted. Warming can accelerate crop development and cause early flowering, maturity, and harvesting, therefore shortening the growing season in croplands (Bai et al., 2019; Liang et al., 2021). Instead of tracking temperature change, farmers may respond to changing precipitation regimes, such as that maize is usually planted when average precipitation and potential evapotranspiration fall within suitable ranges (Sacks et al., 2010). Complex adaptations such as crop rotations (Marini et al., 2020) and hybrid varietal selection for fast growth, high yield, and stress tolerance (Atlin et al., 2017) may lead to climate-phenology decoupling. For example, in the Midwestern US, a significant expansion in maize and soybean cultivation, coupled with decreases in wheat and oats, delayed greenup at a rate of $1.8\text{--}6.7 \text{ day decade}^{-1}$ during 1982–2014 (Zhang et al., 2019). Failure to take advantage of the warming-induced extension of the potential growing season may give rise to a novel yield gap (Lobell et al., 2009) under climate change, leading to a missed opportunity to enhance productivity and pose challenges to achieving food security. On the other hand, active management of the agricultural landscape can help maintain the relationship between phenology and changing climate. For instance, maize and soybeans in the US advanced in planting dates and lengthened growing seasons from 1981 to 2005 due to increased growing degree day accumulation (Sacks & Kucharik, 2011). In northeastern China, the negative impact of a warming-induced shortened rice growth period was partly offset by earlier sowing dates and the adoption of cultivars with a longer growth period (Bai et al., 2019). With further studies on the crop yield and economic consequences of the climate-phenology mismatch, agricultural managers can better optimize sowing dates and crop varieties. In the long term, assessments of climate-phenology mismatch can help design crop ideotypes and guide crop breeding to further expand the toolbox for agro-adaptation.

The relationship between phenological shifts and climate change in semi-natural lands varies greatly over space (Figure 3b). For example, although forests in New England in the Northeastern United States have been reported to have lengthened their growing season as a result of warming (Janowiak et al., 2018) our analysis suggests otherwise, with most of the area having experienced a decrease in growing season length (arrows in New England point to the south in Figure 2b). It should be noted that previous studies have mostly focused on mono-specific forests at a local scale, but satellite-observed phenology also captures phenological change induced by species compositional changes, such as the dramatic reduction in evergreen hemlock caused by introduced pathogens (Knighton et al., 2019) and the replacement of spruce-fir forests with maple-beech-birch and oak-hickory forests (Alig & Butler, 2004) in the northeastern US. Large-scale afforestation and reforestation programs, such as the Three-North Shelter Forest Program in Northeastern China (Lu et al., 2018), can significantly alter land surface phenology, possibly extending the growing season and mitigating climate-phenology mismatch. The influence of timberland management on phenology and corresponding adaptive strategies under climate change has rarely been examined and deserves further investigation.

Given the small number of pixels with human settlements as the dominant land use in the study area, we could not test the net effect of land use changes like urbanization, on climate-phenology mismatch. Nevertheless, phenological shifts in urban areas may be desynchronized from regional climate patterns due to urban heat island effects (S. Wang et al., 2019), CO_2 fertilization (S. Wang et al., 2019), irrigation (Buyantuyev & Wu, 2012), and the introduction of non-native species (Buyantuyev & Wu, 2012). Larger-scale changes in plant phenology might be observed in the future, given the rapid expansion of urban areas.

This study provides one of the first quantifications of continental-scale widespread phenological mismatch, especially in human-dominated landscapes. Looking forward, a concerted effort will be needed to further establish the mechanisms and consequences of phenological mismatch. First, the scaling of phenological mismatch at finer resolutions should be investigated, as phenology is highly heterogeneous and mediated by local microclimate variables in complex terrain (Villegas et al., 2010; Ward et al., 2018). Second, insights from land surface phenology in this study can be enhanced by the inclusion of individual-to species-level phenology data that are free of confounding factors such as species composition, disturbance, and snow (C. Wang et al., 2017). Last, the relationship between measurements of phenological mismatch and fitness measurements, such as productivity and stress, needs to be tested systematically, extending beyond several classic examples of interacting species (Visser & Both, 2005). Although these efforts are currently limited by the lack of long-term phenology observations and fitness measurements, future data collection may enable us to more rigorously test well-known ecological theories about phenological mismatch, to more sustainably manage plant species and mitigate the pernicious impacts of climate change.

5. Conclusions

Plant phenology is expected to closely track the changing climate, but this phenology-climate coupling might be disrupted by human activities during rapid climate change. While studies have revealed the possibility of climate-phenology decoupling, until now we lack a systematic quantification of this mismatch and its correlation with anthropogenic activities. Our findings confirm that land surface phenology changed rapidly over the past three decades in northern mid-to high-latitudes. Our results show that, however, the movement of phenology isolines outpaced that of temperature isolines in wildlands but lagged behind those in anthropogenic landscapes. Anthropogenic activities are not only associated with the slower movement of phenology isolines, but also an increased climate-phenology mismatch. A stable relationship between land surface phenology and climate in human-dominated landscapes is critical to maintaining biodiversity and increasing ecosystem productivity. Our study demonstrates a coherent approach to quantify climate-phenology mismatches and understand their spatial pattern. Insights from these findings help guide sustainable management strategy through the optimized selection of species and planting practices in the human-dominated Earth.

Conflict of Interest

The authors declare no conflicts of interest relevant to this study.

Data Availability Statement

All the data and code are publicly available to fully reproduce the results. The Climate Research Unit (CRU) time-series (TS) data set v. 4.03 is available at https://crudata.uea.ac.uk/cru/data/hrg/cru_ts_4.03/. The VIPPHEN EVI2 Phenology data product v. 4.1 is available at https://lpdaac.usgs.gov/products/vipphen_evi2v004/. The Anthromes v. 2 data were retrieved from <http://ecotope.org/anthromes/v2/>, while the Gridded Population of the World data v. 4 were retrieved from <https://sedac.ciesin.columbia.edu/data/set/gpw-v4-population-density-rev11>. Ground observations of plant phenology are from the USA-National Phenology Network database, available at <https://www.usanpn.org/data/observational>. The R code of the calculation of climate-phenology metrics, comparison between land uses, regression analyses against the human population density, and ground observation analyses are available at <https://doi.org/10.5281/zenodo.5576375>.

References

- Alig, R. J., & Butler, B. J. (2004). *Area changes for forest cover types in the United States, 1952 to 1997, with projections to 2050. (PNW-GTR-613; p. PNW-GTR-613)*. U.S. Department of Agriculture, Forest Service, Pacific Northwest Research Station. <https://doi.org/10.2737/PNW-GTR-613>
- Andela, N., Morton, D. C., Giglio, L., Chen, Y., Werf, G. R., van der Kasibhatla, P. S., et al. (2017). A human-driven decline in global burned area. *Science*, 356(6345), 1356–1362. <https://doi.org/10.1126/science.aal4108>
- Atlin, G. N., Cairns, J. E., & Das, B. (2017). Rapid breeding and varietal replacement are critical to adaptation of cropping systems in the developing world to climate change. *Global Food Security*, 12, 31–37. <https://doi.org/10.1016/j.gfs.2017.01.008>
- Bai, H., Xiao, D., Zhang, H., Tao, F., & Hu, Y. (2019). Impact of warming climate, sowing date, and cultivar shift on rice phenology across China during 1981–2010. *International Journal of Biometeorology*, 63(8), 1077–1089. <https://doi.org/10.1007/s00484-019-01723-z>

Acknowledgments

For comments on the manuscript, we thank Elliot Campbell, Greg Gilbert, Adam Millard-Ball, Bijan Seyednasrollah, and members of the Zhu Lab at the University of California, Santa Cruz (UCSC). This study was supported by the UCSC Regents' Fellowship, the UCSC Hammett Fellowship, and the Microsoft AI for Earth Grant to Y. Song, the NASA Carbon Science program (Grant # NNX-17AE69G) to T. Hwang, and the UCSC Committee on Research Faculty Research Grant and NSF DEB Grant 2045309 (CAREER) to K. Zhu.

- Bauerle, W. L., Oren, R., Way, D. A., Qian, S. S., Stoy, P. C., Thornton, P. E., et al. (2012). Photoperiodic regulation of the seasonal pattern of photosynthetic capacity and the implications for carbon cycling. *Proceedings of the National Academy of Sciences*, *109*(22), 8612–8617. <https://doi.org/10.1073/pnas.1119131109>
- Burrows, M. T., Schoeman, D. S., Buckley, L. B., Moore, P., Poloczanska, E. S., Brander, K. M., et al. (2011). The pace of shifting climate in marine and terrestrial ecosystems. *Science*, *334*(6056), 652–655. <https://doi.org/10.1126/science.1210288>
- Buyantuyev, A., & Wu, J. (2012). Urbanization diversifies land surface phenology in arid environments: Interactions among vegetation, climatic variation, and land use pattern in the Phoenix metropolitan region, USA. *Landscape and Urban Planning*, *105*(1), 149–159. <https://doi.org/10.1016/j.landurbplan.2011.12.013>
- Center For International Earth Science Information Network-CIESIN-Columbia University. (2018). *Gridded population of the World, version 4 (GPWv4): Population density, revision 11 [data set]*: NASA Socioeconomic Data and Applications Center (SEDAC). <https://doi.org/10.7927/h49c6vhw>
- Cornelius, C., Estrella, N., Franz, H., & Menzel, A. (2013). Linking altitudinal gradients and temperature responses of plant phenology in the Bavarian Alps. *Plant Biology*, *15*(s1), 57–69. <https://doi.org/10.1111/j.1438-8677.2012.00577.x>
- Cushing, D. H. (1969). The regularity of the spawning season of some fishes. *ICES Journal of Marine Science*, *33*(1), 81–92. <https://doi.org/10.1093/icesjms/33.1.81>
- de Beurs, K. M., & Henebry, G. M. (2008). War, drought, and phenology: Changes in the land surface phenology of Afghanistan since 1982. *Journal of Land Use Science*, *3*(2–3), 95–111. <https://doi.org/10.1080/17474230701786109>
- Delpierre, N., Dufréne, E., Soudani, K., Ulrich, E., Cecchini, S., Boé, J., & François, C. (2009). Modelling interannual and spatial variability of leaf senescence for three deciduous tree species in France. *Agricultural and Forest Meteorology*, *149*(6), 938–948. <https://doi.org/10.1016/j.agrformet.2008.11.014>
- Didan, K., & Barreto, A. (2016). *NASA MEaSUREs Vegetation Index and Phenology (VIP) Phenology EVI2 Yearly Global 0.05Deg CMG [Data set]*. NASA EOSDIS Land Processes DAAC. https://doi.org/10.5067/measures/vip/vipphen_evi2.004
- Duncan, J. M. A., Dash, J., & Atkinson, P. M. (2015). The potential of satellite-observed crop phenology to enhance yield gap assessments in smallholder landscapes. *Frontiers in Environmental Science*, *3*. <https://doi.org/10.3389/fenvs.2015.00056>
- Duputié, A., Rutschmann, A., Ronce, O., & Chuine, I. (2015). Phenological plasticity will not help all species adapt to climate change. *Global Change Biology*, *21*(8), 3062–3073. <https://doi.org/10.1111/gcb.12914>
- Ellis, E. C., Goldewijk, K. K., Siebert, S., Lightman, D., & Ramankutty, N. (2010). Anthropogenic transformation of the biomes, 1700 to 2000. *Global Ecology and Biogeography*, *19*(5), 589–606. <https://doi.org/10.1111/j.1466-8238.2010.00540.x>
- Elmendorf, S. C., Jones, K. D., Cook, B. I., Diez, J. M., Enquist, C. A. F., Hufft, R. A., et al. (2016). The plant phenology monitoring design for The National Ecological Observatory Network. *Ecosphere*, *7*, e01303. <https://doi.org/10.1002/ecs2.1303>
- Elmore, A. J., Guinn, S. M., Minsley, B. J., & Richardson, A. D. (2012). Landscape controls on the timing of spring, autumn, and growing season length in mid-Atlantic forests. *Global Change Biology*, *18*(2), 656–674. <https://doi.org/10.1111/j.1365-2486.2011.02521.x>
- Finley, A. O., Banerjee, S., & Gelfand, A. E. (2013). *SpBayes for large univariate and multivariate point-referenced spatio-temporal data models*. *ArXiv:1310.8192 [Stat]*. Retrieved from <http://arxiv.org/abs/1310.8192>
- Finley, A. O., Banerjee, S., & Gelfand, A. E. (2015). SpBayes for large univariate and multivariate point-referenced spatio-temporal data models. *Journal of Statistical Software*, *63*(1), 1–28. <https://doi.org/10.18637/jss.v063.i13>
- Fridley, J. D. (2012). Extended leaf phenology and the autumn niche in deciduous forest invasions. *Nature*, *485*(7398), 359–362. <https://doi.org/10.1038/nature11056>
- Fu, Y. H., Piao, S., Zhou, X., Geng, X., Hao, F., Vitasse, Y., & Janssens, I. A. (2019). Short photoperiod reduces the temperature sensitivity of leaf-out in saplings of *Fagus sylvatica* but not in horse chestnut. *Global Change Biology*, *25*(5), 1696–1703. <https://doi.org/10.1111/gcb.14599>
- Fu, Y. H., Zhang, X., Piao, S., Hao, F., Geng, X., Vitasse, Y., et al. (2019). Daylength helps temperate deciduous trees to leaf-out at the optimal time. *Global Change Biology*, *25*(7), 2410–2418. <https://doi.org/10.1111/gcb.14633>
- Fu, Y. H., Zhao, H., Piao, S., Peaucelle, M., Peng, S., Zhou, G., et al. (2015). Declining global warming effects on the phenology of spring leaf unfolding. *Nature*, *526*(7571), 104–107. <https://doi.org/10.1038/nature15402>
- Gao, F., Anderson, M. C., Zhang, X., Yang, Z., Alfieri, J. G., Kustas, W. P., et al. (2017). Toward mapping crop progress at field scales through fusion of Landsat and MODIS imagery. *Remote Sensing of Environment*, *188*, 9–25. <https://doi.org/10.1016/j.rse.2016.11.004>
- Hällfors, M. H., Pöyry, J., Heliölä, J., Kohonen, I., Kuussaari, M., Leinonen, R., et al. (2021). Combining range and phenology shifts offers a winning strategy for boreal Lepidoptera. *Ecology Letters*, *24*, 1619–1632. <https://doi.org/10.1111/ele.13774>
- Hamann, A., Roberts, D. R., Barber, Q. E., Carroll, C., & Nielsen, S. E. (2015). Velocity of climate change algorithms for guiding conservation and management. *Global Change Biology*, *21*(2), 997–1004. <https://doi.org/10.1111/gcb.12736>
- Harris, I., Jones, P. D., Osborn, T. J., & Lister, D. H. (2014). Updated high-resolution grids of monthly climatic observations—The CRU TS3.10 Dataset. *International Journal of Climatology*, *34*(3), 623–642. <https://doi.org/10.1002/joc.3711>
- Helman, D. (2018). Land surface phenology: What do we really ‘see’ from space? *The Science of the Total Environment*, *618*, 665–673. <https://doi.org/10.1016/j.scitotenv.2017.07.237>
- Hopkins, A. D. (1918). Periodical events and natural law as guides to agricultural research and practice. *Monthly Weather Review*, *9*, 1–42.
- Huang, M., Piao, S., Janssens, I. A., Zhu, Z., Wang, T., Wu, D., et al. (2017). Velocity of change in vegetation productivity over northern high latitudes. *Nature Ecology & Evolution*, *1*(11), 1649–1654. <https://doi.org/10.1038/s41559-017-0328-y>
- Hwang, T., Band, L. E., Miniati, C. F., Song, C., Bolstad, P. V., Vose, J. M., & Love, J. P. (2014). Divergent phenological response to hydroclimate variability in forested mountain watersheds. *Global Change Biology*, *20*(8), 2580–2595. <https://doi.org/10.1111/gcb.12556>
- Hwang, T., Song, C., Vose, J., & Band, L. (2011). Topography-mediated controls on local vegetation phenology estimated from MODIS vegetation index. *Landscape Ecology*, *26*, 541–556. <https://doi.org/10.1007/s10980-011-9580-8>
- Janowiak, M. K., D’Amato, A. W., Swanston, C. W., Iverson, L., Thompson, F. R., Dijk, W. D., et al. (2018). *New England and northern New York forest ecosystem vulnerability assessment and synthesis: A report from the New England Climate Change Response Framework project*. <https://doi.org/10.2737/nrs-gtr-173>
- Kariyeva, J., & van Leeuwen, W. J. D. (2012). Phenological dynamics of irrigated and natural drylands in Central Asia before and after the USSR collapse. *Agriculture, Ecosystems & Environment*, *162*, 77–89. <https://doi.org/10.1016/j.agee.2012.08.006>
- Keenan, T. F., Richardson, A. D., & Hufkens, K. (2020). On quantifying the apparent temperature sensitivity of plant phenology. *New Phytologist*, *225*(2), 1033–1040. <https://doi.org/10.1111/nph.16114>
- Kharouba, H. M., & Wolkovich, E. M. (2020). Disconnects between ecological theory and data in phenological mismatch research. *Nature Climate Change*, *10*(5), 406–415. <https://doi.org/10.1038/s41558-020-0752-x>

- Knighton, J., Conneely, J., & Walter, M. T. (2019). Possible increases in flood frequency due to the loss of Eastern Hemlock in the North-eastern United States: Observational insights and predicted impacts. *Water Resources Research*, 55(7), 5342–5359. <https://doi.org/10.1029/2018WR024395>
- Körner, C., & Basler, D. (2010). Phenology under global warming. *Science*, 327(5972), 1461–1462. <https://doi.org/10.1126/science.1186473>
- Laskin, D. N., McDermid, G. J., Nielsen, S. E., Marshall, S. J., Roberts, D. R., & Montagni, A. (2019). Advances in phenology are conserved across scale in present and future climates. *Nature Climate Change*, 9(5), 419–425. <https://doi.org/10.1038/s41558-019-0454-4>
- Lenoir, J., Bertrand, R., Comte, L., Bourgeaud, L., Hattab, T., Muriene, J., & Grenouillet, G. (2020). Species better track climate warming in the oceans than on land. *Nature Ecology & Evolution*, 4(8), 1044–1059. <https://doi.org/10.1038/s41559-020-1198-2>
- Li, X., Zhou, Y., Asrar, G. R., Mao, J., Li, X., & Li, W. (2017). Response of vegetation phenology to urbanization in the conterminous United States. *Global Change Biology*, 23(7), 2818–2830. <https://doi.org/10.1111/gcb.13562>
- Liang, L., Henebry, G. M., Liu, L., Zhang, X., & Hsu, L. C. (2021). Trends in land surface phenology across the conterminous United States (1982–2016) analyzed by NEON domains. *Ecological Applications*, 31(5), e02323. <https://doi.org/10.1002/eap.2323>
- Loarie, S. R., Duffy, P. B., Hamilton, H., Asner, G. P., Field, C. B., & Ackerly, D. D. (2009). The velocity of climate change. *Nature*, 462(7276), 1052–1055. <https://doi.org/10.1038/nature08649>
- Lobell, D. B., Cassman, K. G., & Field, C. B. (2009). Crop Yield Gaps: Their importance, magnitudes, and causes. *Annual Review of Environment and Resources*, 34(1), 179–204. <https://doi.org/10.1146/annurev.enviro.041008.093740>
- Lu, F., Hu, H., Sun, W., Zhu, J., Liu, G., Zhou, W., et al. (2018). Effects of national ecological restoration projects on carbon sequestration in China from 2001 to 2010. *Proceedings of the National Academy of Sciences*, 115(16), 4039–4044. <https://doi.org/10.1073/pnas.1700294115>
- Marini, L., St-Martin, A., Vico, G., Baldoni, G., Berti, A., Blecharczyk, A., et al. (2020). Crop rotations sustain cereal yields under a changing climate. *Environmental Research Letters*, 15(12), 124011. <https://doi.org/10.1088/1748-9326/abc651>
- Menzel, A., Yuan, Y., Matiu, M., Sparks, T., Scheiffinger, H., Gehrig, R., & Estrella, N. (2020). Climate change fingerprints in recent European plant phenology. *Global Change Biology*, 26(4), 2599–2612. <https://doi.org/10.1111/gcb.15000>
- Miao, L., Müller, D., Cui, X., & Ma, M. (2017). Changes in vegetation phenology on the Mongolian Plateau and their climatic determinants. *PLoS One*, 12, e0190313. <https://doi.org/10.1371/journal.pone.0190313>
- Molinos, J. G., Schoeman, D. S., Brown, C. J., & Burrows, M. T. (2019). VoCC: An R package for calculating the velocity of climate change and related climatic metrics. *Methods in Ecology and Evolution*, 10(12), 2195–2202. <https://doi.org/10.1111/2041-210X.13295>
- Morin, X., Viner, D., & Chuine, I. (2008). Tree species range shifts at a continental scale: New predictive insights from a process-based model. *Journal of Ecology*, 96(4), 784–794. <https://doi.org/10.1111/j.1365-2745.2008.01369.x>
- O’Leary, D., Inouye, D., Dubayah, R., Huang, C., & Hurr, G. (2020). Snowmelt velocity predicts vegetation green-wave velocity in mountainous ecological systems of North America. *International Journal of Applied Earth Observation and Geoinformation*, 89, 102110. <https://doi.org/10.1016/j.jag.2020.102110>
- Ordóñez, A., Williams, J. W., & Svenning, J.-C. (2016). Mapping climatic mechanisms likely to favour the emergence of novel communities. *Nature Climate Change*, 6(12), 1104–1109. <https://doi.org/10.1038/nclimate3127>
- Ovaskainen, O., Skorokhodova, S., Yakovleva, M., Sukhov, A., Kutenkov, A., Kutenkova, N., et al. (2013). Community-level phenological response to climate change. *Proceedings of the National Academy of Sciences*, 110(33), 13434–13439. <https://doi.org/10.1073/pnas.1305533110>
- Parmesan, C., & Yohe, G. (2003). A globally coherent fingerprint of climate change impacts across natural systems. *Nature*, 421(6918), 37–42. <https://doi.org/10.1038/nature01286>
- Peng, J., Wu, C., Zhang, X., Wang, X., & Gonsamo, A. (2019). Satellite detection of cumulative and lagged effects of drought on autumn leaf senescence over the Northern Hemisphere. *Global Change Biology*, 25(6), 2174–2188. <https://doi.org/10.1111/gcb.14627>
- Ralhan, P. K., Khanna, R. K., Singh, S. P., & Singh, J. S. (1985). Phenological characteristics of the tree layer of Kumaun Himalayan forests. *Vegetatio*, 60(2), 91–101. JSTOR. <https://doi.org/10.1007/bf00040351>
- R Core Team. (2019). *R: A language and environment for statistical computing*: R foundation for statistical computing. Retrieved from <https://www.r-project.org/>
- Reed, T. E., Jenouvrier, S., & Visser, M. E. (2013). Phenological mismatch strongly affects individual fitness but not population demography in a woodland passerine. *Journal of Animal Ecology*, 82(1), 131–144. <https://doi.org/10.1111/j.1365-2656.2012.02020.x>
- Ren, S., Yi, S., Peichl, M., & Wang, X. (2018). Diverse responses of vegetation phenology to climate change in different grasslands in inner Mongolia during 2000–2016. *Remote Sensing*, 10(1), 17. <https://doi.org/10.3390/rs10010017>
- Richardson, A. D., Bailey, A. S., Denny, E. G., Martin, C. W., & O’keefe, J. (2006). Phenology of a northern hardwood forest canopy. *Global Change Biology*, 12(7), 1174–1188. <https://doi.org/10.1111/j.1365-2486.2006.01164.x>
- Richardson, A. D., Hufkens, K., Milliman, T., Aubrecht, D. M., Furze, M. E., Seyednasrollah, B., et al. (2018). Ecosystem warming extends vegetation activity but heightens vulnerability to cold temperatures. *Nature*, 560(7718), 368–371. <https://doi.org/10.1038/s41586-018-0399-1>
- Richardson, B. A., Chaney, L., Shaw, N. L., & Still, S. M. (2017). Will phenotypic plasticity affecting flowering phenology keep pace with climate change? *Global Change Biology*, 23(6), 2499–2508. <https://doi.org/10.1111/gcb.13532>
- Roetzer, T., Witzenzeller, M., Haeckel, H., & Nekovar, J. (2000). Phenology in central Europe—Differences and trends of spring phenophases in urban and rural areas. *International Journal of Biometeorology*, 44(2), 60–66. <https://doi.org/10.1007/s004840000062>
- Sacks, W. J., Deryng, D., Foley, J. A., & Ramankutty, N. (2010). Crop planting dates: An analysis of global patterns. *Global Ecology and Biogeography*, 19(5), 607–620. <https://doi.org/10.1111/j.1466-8238.2010.00551.x>
- Sacks, W. J., & Kucharik, C. J. (2011). Crop management and phenology trends in the U.S. Corn Belt: Impacts on yields, evapotranspiration and energy balance. *Agricultural and Forest Meteorology*, 151(7), 882–894. <https://doi.org/10.1016/j.agrformet.2011.02.010>
- Sakamoto, T., Yokozawa, M., Toritani, H., Shibayama, M., Ishitsuka, N., & Ohno, H. (2005). A crop phenology detection method using time-series MODIS data. *Remote Sensing of Environment*, 96(3), 366–374. <https://doi.org/10.1016/j.rse.2005.03.008>
- Soolanayakanahally, R. Y., Guy, R. D., Silim, S. N., & Song, M. (2013). Timing of photoperiodic competency causes phenological mismatch in balsam poplar (*Populus balsamifera* L.). *Plant, Cell & Environment*, 36(1), 116–127. <https://doi.org/10.1111/j.1365-3040.2012.02560.x>
- Tao, F., Yokozawa, M., Zhang, Z., Hayashi, Y., & Ishigooka, Y. (2008). Land surface phenology dynamics and climate variations in the North East China Transect (NECT), 1982–2000. *International Journal of Remote Sensing*, 29(19), 5461–5478. <https://doi.org/10.1080/01431160801908103>
- Villegas, J. C., Breshears, D. D., Zou, C. B., & Royer, P. D. (2010). Seasonally pulsed heterogeneity in microclimate: Phenology and cover effects along deciduous grassland–forest continuum. *Vadose Zone Journal*, 9(3), 537–547. <https://doi.org/10.2136/vzj2009.0032>
- Visser, M. E., & Both, C. (2005). Shifts in phenology due to global climate change: The need for a yardstick. *Proceedings of the Royal Society B. Biological Science*, 272(1581), 2561–2569. <https://doi.org/10.1098/rspb.2005.3356>
- Vitasse, Y., François, C., Delpierre, N., Dufrene, E., Kremer, A., Chuine, I., & Delzon, S. (2011). Assessing the effects of climate change on the phenology of European temperate trees. *Agricultural and Forest Meteorology*, 151(7), 969–980. <https://doi.org/10.1016/j.agrformet.2011.03.003>

- Wang, C., Chen, J., Wu, J., Tang, Y., Shi, P., Black, T. A., & Zhu, K. (2017). A snow-free vegetation index for improved monitoring of vegetation spring green-up date in deciduous ecosystems. *Remote Sensing of Environment*, 196, 1–12. <https://doi.org/10.1016/j.rse.2017.04.031>
- Wang, S., Ju, W., Peñuelas, J., Cescatti, A., Zhou, Y., Fu, Y., et al. (2019). Urban–rural gradients reveal joint control of elevated CO₂ and temperature on extended photosynthetic seasons. *Nature Ecology & Evolution*, 3(7), 1076–1085. <https://doi.org/10.1038/s41559-019-0931-1>
- Wang, X., Xiao, J., Li, X., Cheng, G., Ma, M., Zhu, G., et al. (2019). No trends in spring and autumn phenology during the global warming hiatus. *Nature Communications*, 10(1), 2389. <https://doi.org/10.1038/s41467-019-10235-8>
- Ward, D. F. L., Wotherspoon, S., Melbourne-Thomas, J., Haapkylä, J., & Johnson, C. R. (2018). Detecting ecological regime shifts from transect data. *Ecological Monographs*, 88(4), 694–715. <https://doi.org/10.1002/ecm.1312>
- Wheeler, H. C., Høye, T. T., Schmidt, N. M., Svenning, J.-C., & Forchhammer, M. C. (2015). Phenological mismatch with abiotic conditions—Implications for flowering in Arctic plants. *Ecology*, 96(3), 775–787. <https://doi.org/10.1890/14-0338.1>
- White, M. A., Beurs, K. M. D., Didan, K., Inouye, D. W., Richardson, A. D., Jensen, O. P., et al. (2009). Intercomparison, interpretation, and assessment of spring phenology in North America estimated from remote sensing for 1982–2006. *Global Change Biology*, 15(10), 2335–2359. <https://doi.org/10.1111/j.1365-2486.2009.01910.x>
- Zhang, X., Liu, L., & Henebry, G. M. (2019). Impacts of land cover and land use change on long-term trend of land surface phenology: A case study in agricultural ecosystems. *Environmental Research Letters*, 14(4), 044020. <https://doi.org/10.1088/1748-9326/ab04d2>
- Zhu, K., Woodall, C. W., & Clark, J. S. (2012). Failure to migrate: Lack of tree range expansion in response to climate change. *Global Change Biology*, 18(3), 1042–1052. <https://doi.org/10.1111/j.1365-2486.2011.02571.x>
- Zhu, W., Tian, H., Xu, X., Pan, Y., Chen, G., & Lin, W. (2012). Extension of the growing season due to delayed autumn over mid and high latitudes in North America during 1982–2006. *Global Ecology and Biogeography*, 21(2), 260–271. <https://doi.org/10.1111/j.1466-8238.2011.00675.x>
- Zohner, C. M., Benito, B. M., Svenning, J.-C., & Renner, S. S. (2016). Day length unlikely to constrain climate-driven shifts in leaf-out times of northern woody plants. *Nature Climate Change*, 6(12), 1120–1123. <https://doi.org/10.1038/nclimate3138>

References From the Supporting Information

- Blois, J. L., Williams, J. W., Fitzpatrick, M. C., Jackson, S. T., & Ferrier, S. (2013). Space can substitute for time in predicting climate-change effects on biodiversity. *Proceedings of the National Academy of Sciences*, 110(23), 9374–9379. <https://doi.org/10.1073/pnas.1220228110>
- Friedl, M., Sulla-Menashe, D. (2015). *MCD12C1 MODIS/Terra+Aqua Land Cover Type Yearly L3 Global 0.05Deg CMG V006 [Data set]*. NASA EOSDIS land processes DAAC. <https://doi.org/10.5067/MODIS/MCD12C1.006>
- Peres- Neto, P. R., & Legendre, P. (2010). Estimating and controlling for spatial structure in the study of ecological communities. *Global Ecology and Biogeography*, 19(2), 174–184. <https://doi.org/10.1111/j.1466-8238.2009.00506.x>